UNIVERSITY OF BIRMINGHAM

Research at Birmingham

Technical feasibility study of passive and active cooling for concentrator PV in harsh environment

Aldossary, Abdulrahman; Mahmoud, Saad; Al-Dadah, Raya

Link to publication on Research at Birmingham portal

Accepted Manuscript

Technical Feasibility study of passive and active cooling for Concentrator PV in harsh environment

A. Aldossary[a], S. Mahmoud and R. AL-Dadah

[a]School of Mechanical Engineering, University of Birmingham, Edgbaston, Birmingham, United Kingdom. B15-2TT
axa281@bham.ac.uk, 01212189744

Abstract

Concentrator PV (CPV) has the potential to replace the expensive PV material with cheaper optical elements which also enhance the overall electrical output. The triple junction III-V solar cells are integrated with CPV systems as they are more efficient, have a better response to high concentration, and lower temperature coefficient. However, using high solar concentration ratios will increase the solar cell surface temperature which is inversely proportional to the PV electrical efficiency. This work investigates the feasibility of passive and active cooling to maintain a single triple junction PV cell surface temperature and electrical performance under high solar concentration in the harsh environment like Saudi Arabia where ambient temperature can reach up to 50° C in summer time. To study the feasibility of passive cooling in such an environment, CPV thermal simulation is undertaken to examine the performance of two heat sink designs namely Round Pin Heat Sink (RPHS) and Straight Fins Heat Sink (SFHS) under different ambient temperatures. The simulation reveals that passive cooling using those two heat sinks with concentration ratio of 500x is insufficient to maintain a single PV surface temperature below the operational limit set by the manufacturer i.e. 80^oC especially at high ambient temperatures which may degrade the life of the solar cell. On the other hand, 0.01 m/s water active cooling simulation results prove its ability to maintain the solar cell surface temperature around 60^oC and electrical efficiency at 39.5% regardless of the ambient temperature. Also, the outlet water average temperature for a single and multiple CPVs were examined and results show that placing 14 single CPVs above the cooling channel will raise the temperature to 90^oC which makes the coupling to a single stage absorption heat pump for cooling demand applicable.

1

1. Introduction

Saudi Arabia has high average yearly global solar radiation of 2200 kWh/m^2 (Alawaji 2001) which makes it a candidate for PV applications, particularly Jubail industrial city (JIC) located at latitude 27.00^{o}N and longitude 49.66^{o}E with yearly average total daily solar radiation on a tilted surface of 5987 Wh/m^2 and clearance index of 0.62. The received solar irradiation in JIC can exceed 1100 W/m^2 especially in summer time when ambient temperature can reach to 50°C (Environmental Protection and Control Department 2013). High ambient temperature is one of the major operational challenges of PV in Saudi Arabia as an experimental study reveals that more than 30% decrease in power generation can be experienced during summer time (Harbi et al. 1998).

Solar PV power has been one of the fastest growing renewable energy technologies and it is anticipated that this technology will play a major role in the future of global electricity generation (Twidell & Weir 2006). The main challenge of using PV is the high initial cost when compared to electricity generated from conventional sources. In order to increase the efficiency of solar power generation and make it more cost effective, different methods have been considered and several approaches have been introduced and investigated. One approach for cost reduction in solar power generation is using mirrors, reflectors or lenses to concentrate the incoming solar irradiation on the PV (Garboushian et al. 1997). Multi-junction (MJ) solar cells are recently favoured over single junction cells to be integrated in CPV systems as they are more efficient, have a better response to high concentration, and lower temperature coefficient. The new technology, III-V generation MJ solar cells, offer high efficiencies exceeding (43%) at high concentration compared to traditional solar cells

2

made of a single layer of semiconductor material (Micheli et al. 2013). High concentration will cause high and non-uniform PV cell surface temperature which reduces the efficiency and power output from the cell and ultimately degrades its life (Baig et al. 2012). Therefore, effective cooling is necessary to dissipate the heat load on the solar cell surface and maintain the peak performance in all conditions. Passive and active cooling are the two possible methods for removing heat from high-illumination photovoltaic cells. Passive cooling methods are more reliable and cost effective due to the absence of moving parts. However, they have lower heat dissipation rates than active cooling systems. Moreover, ambient conditions such as air temperature and wind speed have major influence on the heat dissipation performance (Tan 2013). Active cooling is more efficient in reducing the PV surface temperature and can be more technically feasible if the removed heat by the cooling fluid is utilised in different thermal applications (Al-Amri & Mallick 2013). In the published literature (Royne et al. 2005) describe various passive and active cooling methods which have been incorporated into CPV systems to keep the cell temperature below the operational limit. According to Royne et al. passive cooling can be adequate for single cell geometries for solar irradiation up to 1000 suns since there is a large area available behind the cell for a heat sink. On the other hand, more than one high concentration study concluded that passive cooling is not dissipating enough heat from the cell even when a very large heat sink is used especially in high ambient temperatures (Theristis et al. 2012; Edenburn 1980; Eveloy et al. 2012). Therefore, more investigation has to be undertaken to find the optimum solution for each case of CPV system. The objective of this work is to develop a model able to predict the thermal behaviour of different CPV configurations under passive and active cooling. Also, this work examines the capability of two designed heat sinks, namely RPHS and SFHS, for passive cooling and water active cooling to maintain 1 cm^2 solar cell surface temperature below the operational limit i.e. 80°C under high concentration ratio (500x) and different ambient

3

temperatures i.e. 25°C, 30°C, 35°C, 40°C, 45°C, 50°C. Moreover, the outlet water average temperature is examined to investigate the feasibility of coupling the CPV system to a single stage absorption heat pump for cooling demand.

2. Methodology

In this work, a single solar cell is examined using Finite Element Analysis (FEA) in COMSOL multi-physics software. For passive cooling analysis, two heat sinks were designed using SolidWorks and then exported to COMSOL for thermal simulation. Moreover, a solar cell was placed on a water cooling channel to thermally model the active cooling effect. Heat conduction and convection governing equations were solved simultaneously using conjugate heat transfer physical model.

2.1   Passive and active cooling devices investigated

Aluminium Round Pins Heat Sink (RPHS) is designed to be attached underneath the solar cell to dissipate heat. The round pin heat sink consists of 90x90mm^2 base with 2mm thickness and 144 round pins. Each round pin is 50mm high and 5mm diameter with 2.5mm spacing distance between all the round pins in all directions. Figure 1 shows the solar cell at the centre of the heat sink base and the heat sink assembly.

Aluminium Straight Fins Heat Sink (SFHS) consists of 90x90mm^2 base with 2mm thickness and 30 straight fins. Each fin is 90mm long, 50mm high and 1mm thick with 2mm spacing distance between each straight fin. Figure 2 shows the solar cell at the centre of the heat sink base and the heat sink assembly.

In case of active cooling, the bottom side of the MJ solar cell is attached to 1.5mm thick aluminium rectangular cooling channel with the following dimensions: 328mm length, 30mm width, and 10mm height. The calculated hydraulic diameter of this cooling channel is

4

1.11×10^{-2} m and the water velocity is set to 0.01 m/s. Figure 3 shows the solar cell and the cooling channel assembly.

2.2 Problem definition

AZURSPACE III-V MJ PV cell made of GaInP-GaInAs-Ge and area of $10 \times 10 \text{mm}^2$ has typical electrical efficiency of 41.2% under concentration ratio of 500x ($x=1000\text{W/m}^2$) (AZURSPACE 2014). Figure 4 shows the CPV MJ solar cell assembly which consists of solar cell, two copper layers, a ceramic layer, two by-pass diodes, two electrical terminals, and two side solders; all the previous components were considered in the thermal model besides the thermal paste and the heat sink. The operational temperature range of this solar cell is between 25-80$^\text{o}$C which has to be maintained under very high concentration and different ambient temperatures. The solar radiation energy received by the PV cell is partially used to generate electricity and the rest is converted to heat. The amount of input energy that is converted to heat (q_{heat}) can be calculated using equation 1 (Kerzmann & Schaefer 2012):

$$q_{heat} = q_{rad} \cdot (1 - \eta_{pv}) \cdot \text{CR} \tag{1}$$

where q_{rad} is solar radiation incident on the surface of the PV cell, *CR* is the concentration ratio, and (η_{PV}) is the cell average electrical efficiency given as a function of thermal coefficient ($\beta_{thermal} = 0.047\%$), efficiency at reference temperature ($\eta_{Tref} = 41.2\%$), average PV surface temperature (T_{PV}), and reference temperature $T_{ref} = 298.15\text{K}$ as shown in equation 2 (Skoplaki & Palyvos 2009):

$$\eta_{PV} = 41.2\% - [\beta_{thermal}(T_{PV} - 298.15)] \tag{2}$$

At each iteration in the simulation, the PV cell efficiency, η_{PV}, is calculated from equation 2 from the user input values for $\beta_{thermal}$, η_{Tref}, T_{ref}, and from the COMSOL solved value for the cell temperature, T_{PV}.

5

2.3 Theory and governing equations

All three modes of heat transfer are involved when considering a basic CPV assembly i.e. conduction, convection, and radiation. Conjugate heat transfer physical model has the advantage to combine both heat transfer in solids and fluids at the same time. Heat is transferred within the MJ solar cell and its structure by conduction and heat is transferred to the surroundings by both natural and forced convection. Also, some heat is removed from the PV top surface by radiation.

Steady state heat conduction within the PV assembly and to the top surface of the cooling channel is given by Equation (3) below (Theristis et al. 2012; Theristis & O'Donovan 2015).

$$\nabla.(k\nabla T) = 0$$
$$q_{cond} = -k.A.\frac{dT}{dx} \tag{3}$$

Where q_{cond} is the conduction heat-transfer rate (W), A is cross-sectional area (m²), k is the thermal conductivity of the material (W/ (m.K)), and dT/dx is the temperature gradient. The solar energy that is converted to heat will be dissipated from the PV assembly by both natural and forced convection. The CPV assembly is placed on a cooling channel to extract heat from the assembly by forced convection.

The heat loss due to convection on the top and bottom surfaces of CPV assembly is described by Equation (4) (Theristis et al. 2012; Theristis & O'Donovan 2015).

$$q_{conv} = h.A.\Delta T \tag{4}$$

Where q_{conv} is the convection heat-transfer rate (W), h is convection heat transfer coefficient (W/m².k), A is cross-sectional area (m²), and ΔT is temperature difference between fluid and surface (K).

The heat that is lost to the environment due to radiation is given by (5) (Theristis et al. 2012; Theristis & O'Donovan 2015):

$$q_{rad} = \varepsilon.\sigma.A.\left(T_{surf}^4 - T_{amb}^4\right) \tag{5}$$

6

Where q_{rad} is the radiation heat-transfer rate (W), ε is the emissivity of the object, σ is Stefan

Boltzmann constant, and A is area of the object (m^2), T_{surf} is the surface temperature (K), and

T_{amb} is the ambient temperature (K).

The above physical model also solves numerically the heat transfer equations together with

Navier-Stokes equations. For incompressible flow, the continuity (6), momentum (7), and

total energy flux equations (8&9) are listed below:

$$\nabla.(\rho u) = 0 \tag{6}$$

$$\rho u.\nabla u = -\nabla p + \nabla.\left(\mu(\nabla u + (\nabla u)^T)\right) \tag{7}$$

$$e_{tot} = \rho u E_0 - k\nabla T + q_{rad} - \sigma u \tag{8}$$

Where E_0 is the total internal energy and σu the convective stress energy (Bocchi 2015). The

energy balance equation for a stationary study then takes the following form:

$$\int_{\partial \Omega} e_{tot}.\mathrm{n}\,dS = \int_{\Omega} Q_{ext}\,dV \tag{9}$$

Where the left term represents the total net energy rate and the right term represents the total

heat source.

The conduction-convection equation is also solved for the heat transfer in the flowing cooling

water, which is shown in Equation (10) (Teo et al. 2012; Theristis & O'Donovan 2015).

$$\rho C_p u.\nabla T = \nabla.(k\nabla T) \tag{10}$$

In case of active cooling turbulent flow system modelling, the software provides the ability to

run RANS (Reynolds Averaged Navier-Stokes) model and select between the k-ε, k-ω, or

Spalart-Allmaras models. However, in this case the fully developed water velocity is 0.01 m/s

which is equivalent to Reynolds number of about 122 i.e. laminar; therefore Conjugate heat

transfer laminar flow model was chosen for the simulation. Turbulent flow is dissipating heat

more effectively than laminar flow but turbulent flow cause pressure drop in the cooling

7

channel which consumes more power i.e. more costly than laminar flow cooling system. This aspect is crucial when designing and selecting the cooling system.

2.4 Thermal model and assumptions

The solar cell consists of three defined layers namely GaInP, GaInAs, and Ge and the heat flux was uniformly applied on the top surface of GaInP. Under the solar cell there is a highly conductive Al_2O_3 Ceramic sandwiched between two layers of Copper and beneath that there is a thermal paste bonding the cooling channel to the PV assembly.

Figure 4 shows the schematic diagram of the PV assembly that is thermally simulated. The heat input is transferred within the MJ layers by conduction based on the solar cell dimension and thermo-physical properties of each layer. The dimensions and thermo-physical properties of each layer are presented in table 1 and 2 respectively (Theristis et al. 2012; Goldberg 1999).

In order to be able to model these 3D thermal cases, several assumptions and boundary conditions have to be considered (Fontenault & Gutierrez-miravete 2012):

1. The direct solar radiation is considered to be 1000W/m^2 and it was applied uniformly on the PV surface.

2. The applied concentration ratio CR=500x.

3. Therefore the heat flux on the PV cell (1 cm^2) is 500000W/m^2 i.e. 50 W.

4. Range of ambient temperature to be examined: 25°C, 30°C, 35°C, 40°C, 45°C, 50°C.

5. The inlet cooling water temperature for active cooling case is uniform and assumed to be 25°C. Also, the water velocity inside the cooling channel is set to 0.01m/s.

6. The inlet cooling water is fully developed, laminar, steady, and the hydraulic head is enough to fill the cooling channel to ensure that continuous flow of water with no air bubbles (figure 5).

8

7. No slip boundary condition is applied for the internal surfaces of the cooling water channel (figure 5).

8. The cooling channel is not inclined i.e. in horizontal position.

9. The buoyancy force of the cooling water is considered in this CFD model by adding volume force in y-axis to the water domain. The inlet boundary condition is set to (velocity) and the outlet boundary condition is set to (pressure, no viscous stress).

10. All solar irradiation that is not converted to electricity will be developed into heat.

11. The PV is not covered with glass or any other material.

12. No dust or any other deposit is left on the PV surface.

2.5   *Meshing and Solver*

Three different meshing sizes were chosen for this CPV geometry. For the internal wall of the cooling channel where the no slip boundary condition is applied, finer fluid dynamics mesh was selected with minimum and maximum sizes 0.11 and 1.08mm respectively. In addition, the water domain was meshed using fine fluid dynamics mesh where the minimum and maximum sizes are 0.29 and 1.55mm correspondingly. Finally, the remaining geometry including the cooling channel and the PV assembly was meshed utilising fine general physics mesh as the minimum and maximum sizes are 3.28 and 26.20mm respectively. The simulation ran using GMRES (Generalized Minimum Residual) which is an iterative solver to solve general linear systems. Unlike direct solvers, iterative methods approach the solution gradually, rather than in one large computational step. Consequently, when solving a problem with an iterative method, the error estimate in the solution decrease with the number of iterations can be observed (Frei 2013). The relative tolerance of the stationary solver is set to 0.001 by default; this value was reduced to 0.0001 to check if there is more accurate solution but found no difference.

9

3. Results and discussion

In order to validate this thermal model, the worst case scenario where there is no heat sink was simulated and results were compared to the literature. Figure 6 shows that the cell's temperature can reach up to 922^oC at ambient temperature of 25^oC which agrees with the literature as it has been reported that 3x3 mm^2 concentrator solar cell under concentration ratio of 400x and without heat sink the surface temperature can reach to 1200^oC (Min et al. 2009). In case of passive cooling, the generated heat is transferred through the PV cell solid layers by conduction to the heat sinks where it is dissipated by natural convection. Also, some of this heat is radiated back from the cell to the ambient. There are two different geometries are examined here RPHS and SFHS at different ambient temperatures. Figure 7 shows the temperature plot of the solar cell assembly attached to the RPHS; the maximum temperature on the PV surface reaches to 117^oC at ambient temperature of 50^oC. On the other hand, figure 8 shows the temperature profile of the PV assembly attached to SFHS; the maximum temperature is about 96^oC at the same ambient temperature. Although RPHS and SFHS are tested at the same surrounding conditions, SFHS is performing better than RPHS in dissipating heat load with almost constant PV surface temperature difference between the two heat sinks of about 21^oC. It can be concluded that design aspects of the heat sink play a major role in heat dissipation performance. In case of active cooling, the generated heat is transferred through the PV cell solid layers by conduction to the water channel where it is dissipated mainly by forced convection. Figure 9 shows the temperature plot of the PV assembly above the cooling channel at 0.01m/s inlet water velocity corresponding to Reynolds number of around 122; the maximum temperature on the PV surface is about 67^oC at ambient temperature of 50^oC. Clearly, there is a drop in PV surface maximum temperature of about 29^oC compared to SFHS and about 50^oC compared to RPHS.

10

Figure 10 is demonstrating the performance of passive and active cooling in maintaining the PV surface temperature at different ambient conditions; obviously SFHS is dissipating more heat than RPHS in all examined ambient temperatures. For example, at ambient temperature of 25°C the solar cell average surface temperatures are about 65°C and 85°C for SFHS and RPHS respectively while at ambient temperature of 50°C the cell surface average temperatures are about 90°C and 110°C. However, both heat sinks are unable to maintain the PV surface temperature as the ambient temperature increases. On the other hand, water active cooling at moderate velocity of 0.01 m/s has the ability to keep the average surface temperature almost steady at 60°C regardless of the ambient temperature. As a result of increasing PV average surface temperature in case of RPHS and SFHS when ambient temperature increases, the PV electrical efficiency decreases accordingly as illustrated in figure 11. But, active cooling is capable to maintain the output electrical efficiency at 39.5% in different ambient temperatures. Keeping the PV surface temperature within the operating limit specified by the manufacturer is crucial, especially at high concentration and ambient temperatures, to avoid the solar cell life degradation. Figure 12 shows that active cooling is able to maintain the maximum solar cell surface temperature under the operating limit i.e. 80°C at all ambient temperatures. For example, at ambient temperature of 50°C the maximum PV surface does not exceed 68°C. However, RPHS is unable to keep the PV surface temperature below the operating temperature limit at all ambient temperatures. For instance, at ambient temperature of 25°C the maximum PV surface temperature reaches to 91°C. On the other hand, SFHS is capable to maintain the maximum PV surface temperature within the operating limit only at ambient temperature of 25°C and 30°C. But, at ambient temperature of 35°C, 40°C, 45°C, 50°C the maximum PV surface temperature are 80.42^{o}C, 85.63^{o}C, 90.84^{o}C, and 96.06^{o}C respectively. Based on energy conservation principle i.e. input energy equals to the output energy, table 3 is presenting the thermal energy produced by the system at different

11

ambient temperatures where its minor portion wasted to the environment by natural convection and thermal radiation while the major portion carried by the coolant through forced convection. For example, at ambient temperature of 25°C the thermal energy produced is more than 30W about 97% of this energy goes with the forced convection while only 3% is wasted by natural convection and thermal radiation. It can be noticed that at high ambient temperature i.e. 35°C and above the CPV system is gaining heat from the ambient which enhances the thermal performance. For instance, at ambient temperature of 50°C the system is gaining more than 3W through natural convection which added to the forced convection.

Figure 13 shows the water temperature along the cooling channel for a single CPV at different ambient temperatures. At ambient temperature of 50°C, the cooling water average temperature is raised from the input temperature i.e. 25°C to about 30°C while at 25°C ambient temperature the outlet water temperature is increased to 29°C. Moreover, three CPVs were placed on the same cooling channel and thermally simulated to examine the outlet water temperature at the same water velocity and at different ambient temperatures as shown in figure 14. The outlet water average temperature at ambient temperature of 50°C is raised from 25°C to about 39°C. By extrapolating these data, figure 15 is showing that placing 14 CPVs in series on the cooling channel will increase the outlet water average temperature to 90°C even at the lowest tested ambient temperature i.e. 25°C which makes the coupling to a single stage absorption heat pump for cooling demands feasible (Renno & Petito 2013).

4. Thermal model Validation

In order to validate the developed thermal model, Electrical Resistance Heater (ERH) was used to simulate the heat load on the solar cell surface (Wu et al. 2012). PV thermal modelling assumptions are the same as in section 2.5 except that the ambient and cooling water input temperatures are 16.9^{o}C and 15.7^{o}C respectively during the experimental test.

12

Figure 16 shows the temperature profile of the CPV system and the maximum PV surface temperature at ambient temperature of 16.9^oC which reaches to about 55^oC.

Also, table 4 below shows the PV thermal and electrical outputs using equation 1 and 2. The solar irradiation that is not converted to electricity i.e. heat (29.97W) will be applied on the solar cell by placing ERH at the top of the PV assembly as shown in figure 17.

One 35W 15Ω ERH with dimensions of 11.0mm x 10.5mm x 4.5mm having a rated power greater than 29.97W was chosen to simulate the heat load on the PV surface in the CPV system. Variable output power supply was used to control the power input into the resistance heater as shown in figure 18. Five u-shape grooves on the cooling channel (figure 19A) with dimensions of 1.5mm x 0.75mm were made to insert three 0.13mm diameter thermocouples just underneath the PV and two at opposite corners of the PV assembly as shown in figure 19B. Fourteen thermocouples in total were distributed on the CPV system as shown in figure 19 to measure the PV surface temperature, the PV assembly, top of the cooling channel, side of the cooling channel and the cooling water output.

13

Figure 20 shows the close agreement between the experimental and the simulation CPV average surface temperature in different locations. For example, the experimental PV surface temperature is only about 5% higher than the simulation while the coolant outlet temperature of the experimental is almost identical with the simulation results. The CFD predicted cell temperature is used in an electrical model utilising the manufacturer given open circuit voltage, short circuit current, and their temperature coefficients to generate the simulation IV and power curves. Moreover, the experimentally measured cell temperature is used to generate the experimental IV and power curves as shown in figure 21. Due to the close agreement in the average PV surface temperature there is also close agreement in the electrical output between the experimental and the simulation. Therefore, it can be concluded that the developed thermal simulation and the resulted electrical output are verified.

5. Conclusions

Two heat sinks, RPHS and SFHS, attached at the back of a single CPV system were thermally examined to study the feasibility of passive cooling in harsh environment like Saudi Arabia where ambient temperature can be up to 50°C and under high concentration ratio of 500x. Although the PV surface temperature was dropped dramatically after using the two heat sinks compared to the worst case scenario where there is no cooling mechanism i.e. from about 923°C to less than 118°C, the heat dissipation performance was not enough to maintain the PV electrical efficiency and surface temperature especially at high ambient temperatures. SFHS shows better performance than RPHS at all ambient temperatures as SFHS kept the PV surface temperature 21°C lower than RPHS PV surface in all tested ambient temperatures; this is may be due to the difference in design which plays a major role in heat dissipation performance. On the other hand, active cooling at moderate water velocity i.e. 0.01m/s corresponding to Reynolds number of around 122 is able to maintain the PV electrical efficiency at about 39.5% and surface temperature of about 60°C regardless of the

14

ambient temperature. Moreover, active cooling is able to maintain the PV maximum surface temperature under the temperature operating limit set by the manufacturer i.e. 80°C to avoid the solar cell life degradation. Whereas, RPHS is unable to keep the PV surface temperature below the operating limit at all ambient temperatures. Moreover, SFHS is unable to maintain the maximum PV surface temperature within the operating limit at ambient temperature of 35°C and above. Water active cooling is more cost effective if the thermal energy carried by the coolant utilised in a thermal application. Therefore, the water outlet temperature for a single and three CPVs at different ambient temperatures were examined. It was found that outlet water average temperature rose from 25°C to 30°C and from 25°C to about 39°C at ambient temperature of 50°C for a single and three CPVs respectively. By extrapolating theses data the results revealed that placing 14 CPVs on the cooling channel is enough to raise the outlet temperature to 90°C which would make the coupling to a single stage absorption heat pump for cooling demands possible.

6. References

Al-Amri, F. & Mallick, T.K., 2013. Alleviating operating temperature of concentration solar cell by air active cooling and surface radiation. *Applied Thermal Engineering*, 59(1-2), pp.348–354.

Alawaji, S.H., 2001. Evaluation of solar energy research and its applications in Saudi Arabia — 20 years of experience. *Renewable and Sustainable Energy Reviews*, 5(1), pp.59–77.

AZURSPACE, 2014. Enhanced Fresnel Assembly - EFA Type: 3C42A – with 10x10mm^{2} CPV TJ Solar Cell Application: Concentrating Photovoltaic (CPV) Modules. , pp.0–3. Available at: http://www.azurspace.com/images/products/DB_3987-00-00_3C42_AzurDesign_EFA_10x10_2014-03-27.pdf.

Baig, H., Heasman, K.C. & Mallick, T.K., 2012. Non-uniform illumination in concentrating solar cells. *Renewable and Sustainable Energy Reviews*, 16(8), pp.5890–5909.

Bocchi, F., 2015. How to Calculate Mass Conservation and Energy Balance. *COMSOL.* Available at: http://www.comsol.com/blogs/author/fabio-bocchi/ [Accessed January 11, 2016].

15

Edenburn, M.W., 1980. Active and passive cooling for concentrating photovoltaic arrays. In *14th Photovoltaic Specialists Conference*. pp. 771–776.

Environmental Protection and Control Department, 2013. Jubail Industrial City Solar Irradiation.

Eveloy, V., Rodgers, P. & Bojanampati, S., 2012. Enhancement of photovoltaic solar module performance for power generation in the Middle East. *2012 28th Annual IEEE Semiconductor Thermal Measurement and Management Symposium (SEMI-THERM)*, pp.87–97.

Fontenault, B.J. & Gutierrez-miravete, E., 2012. Modeling a Combined Photovoltaic-Thermal Solar Panel.

Frei, W., 2013. Solutions to Linear Systems of Equations: Direct and Iterative Solvers. *COMSOL*. Available at: https://www.comsol.com/blogs/solutions-linear-systems-equations-direct-iterative-solvers/ [Accessed January 11, 2016].

Garboushian, V., Roubideaux, D. & Yoon, S., 1997. Integrated high-concentration PV near-term alternative for low-cost large-scale solar electric power. *Solar Energy Materials and Solar Cells*, 47(1-4), pp.315–323.

Goldberg, Y.A., 1999. Handbook Series on Semiconductor Parameters, Volume 2: Ternary and Quaternary A3B5 Semiconductors. In M. Levinshtein, S. Rumyantsev, & M. Shur, eds. *2*. World Scientific Pub. Co., Inc., pp. 62–88.

Harbi, Y.A.L., Eugenio, N.N. & Zahrani, S.A.L., 1998. photovoltaic-thermal solar energy experiment in saudi arabia. , 5, pp.5–8.

Kerzmann, T. & Schaefer, L., 2012. System simulation of a linear concentrating photovoltaic system with an active cooling system. *Renewable Energy*, 41, pp.254–261.

Micheli, L. et al., 2013. Opportunities and challenges in micro- and nano-technologies for concentrating photovoltaic cooling: A review. *Renewable and Sustainable Energy Reviews*, 20, pp.595–610.

Min, C. et al., 2009. Thermal analysis and test for single concentrator solar cells. *Journal of Semiconductors*, 30(4), p.044011.

Renno, C. & Petito, F., 2013. Design and modeling of a concentrating photovoltaic thermal (CPV/T) system for a domestic application. *Energy and Buildings*, 62, pp.392–402.

Royne, a, Dey, C. & Mills, D., 2005. Cooling of photovoltaic cells under concentrated illumination: a critical review. *Solar Energy Materials and Solar Cells*, 86(4), pp.451–483.

Skoplaki, E. & Palyvos, J. a., 2009. On the temperature dependence of photovoltaic module electrical performance: A review of efficiency/power correlations. *Solar Energy*, 83(5), pp.614–624.

Tan, L., 2013. *Passive Cooling of Concentrated Solar Cells Using Phase Change Material Thermal Storage*. RMIT.

Teo, H.G., Lee, P.S. & Hawlader, M.N. a., 2012. An active cooling system for photovoltaic modules. *Applied Energy*, 90(1), pp.309–315.

Theristis, M. et al., 2012. Design and numerical analysis of enhanced cooling techniques for a high concentration photovoltaic (HCPV) system. *27th European Photovoltaic Solar*

16

Energy Conference and Exhibition, pp.260–265.

Theristis, M. & O'Donovan, T.S., 2015. Electrical-thermal analysis of III–V triple-junction solar cells under variable spectra and ambient temperatures. *Solar Energy*, 118, pp.533–546.

Twidell, J. & Weir, A.D., 2006. *Renewable energy resources*, Taylor & Francis.

Wu, Y. et al., 2012. Experimental characterisation of a Fresnel lens photovoltaic concentrating system. *Solar Energy*, 86(1), pp.430–440.
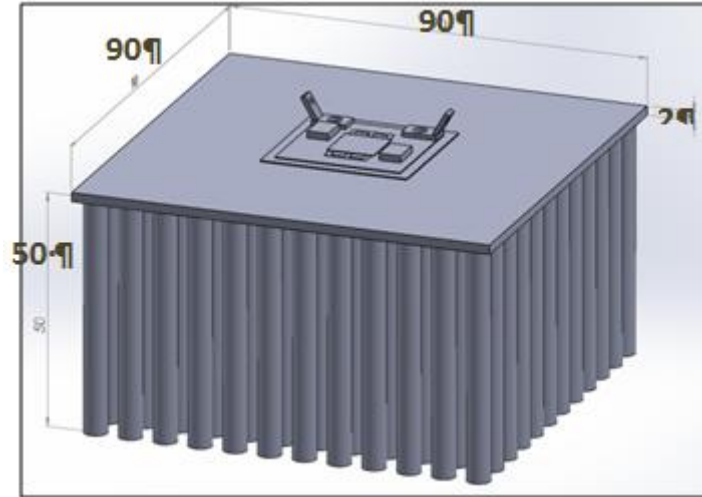
17

Fig.1: Round pins heat sink attached to the solar cell
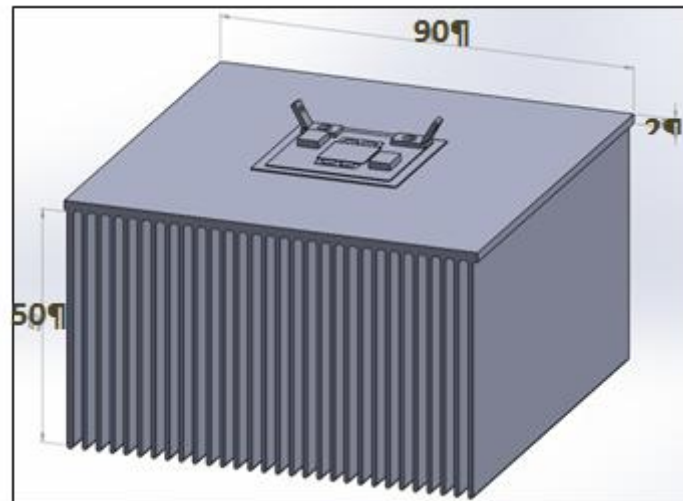
Fig.2: Straight fins heat sink attached to the solar cell

18
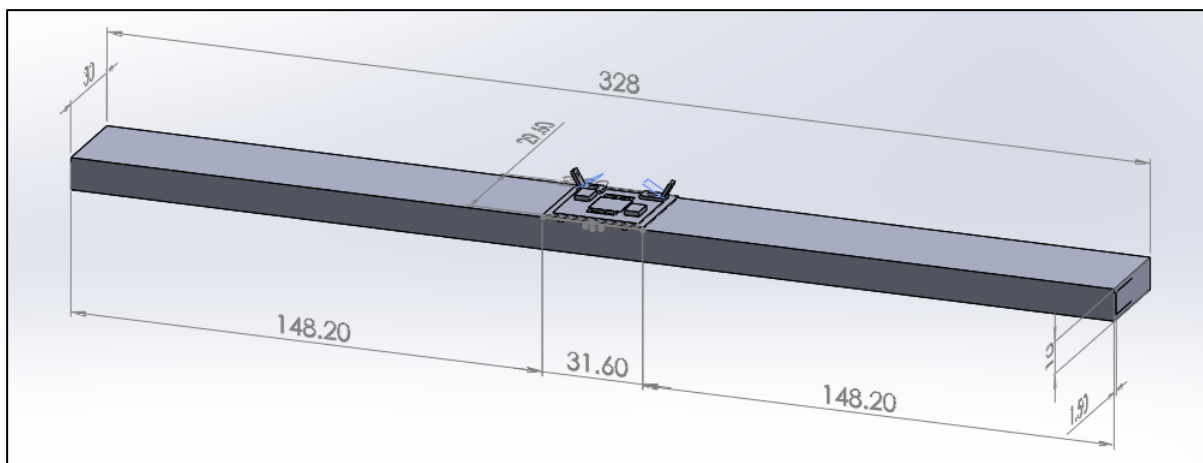
Fig.3: PV assembly attached to the water cooling channel
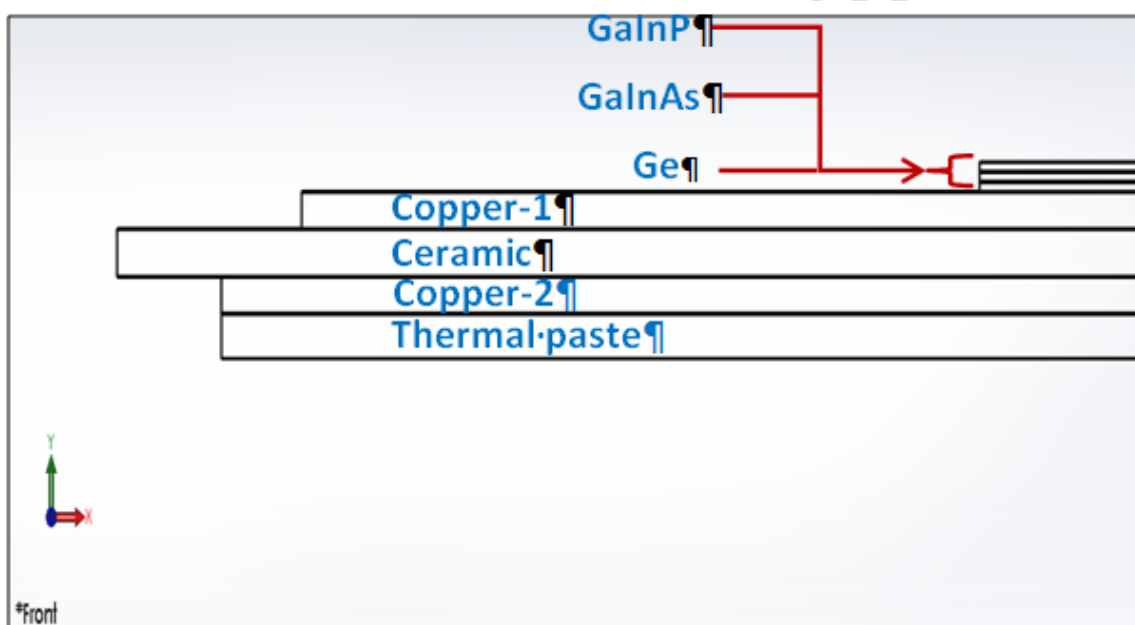
Fig.4: PV assembly layers
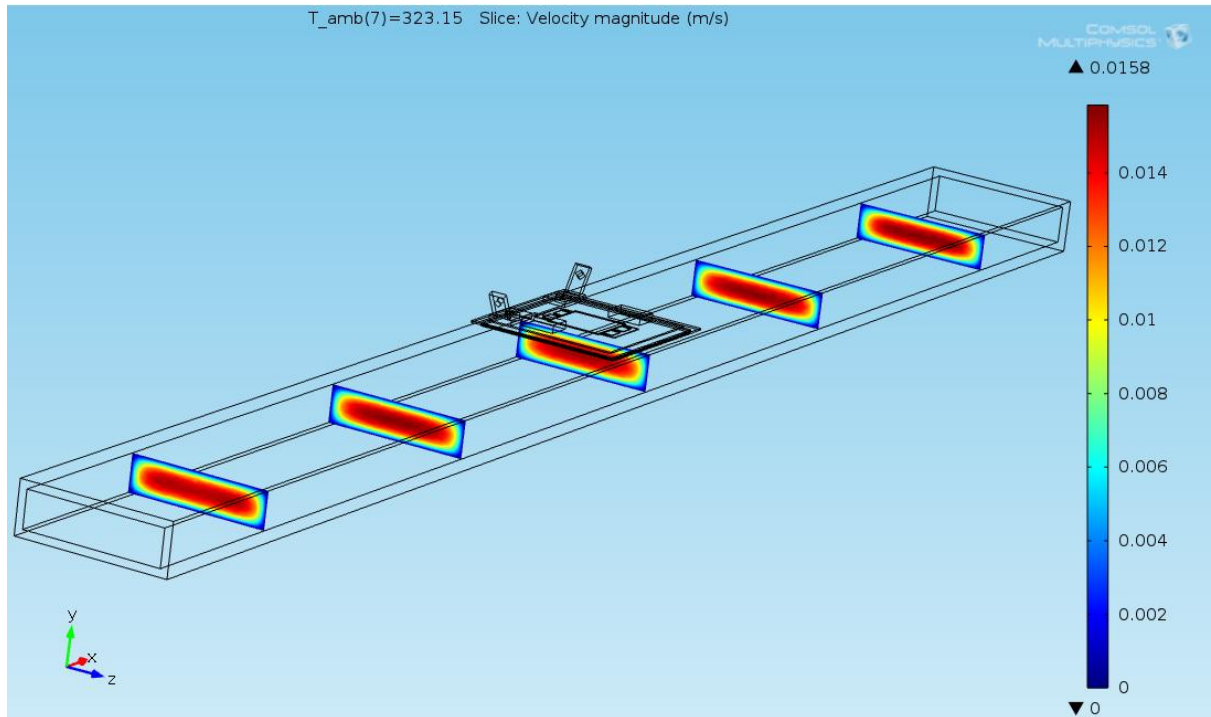
Fig.5: water profile in the cooling channel (m/s)
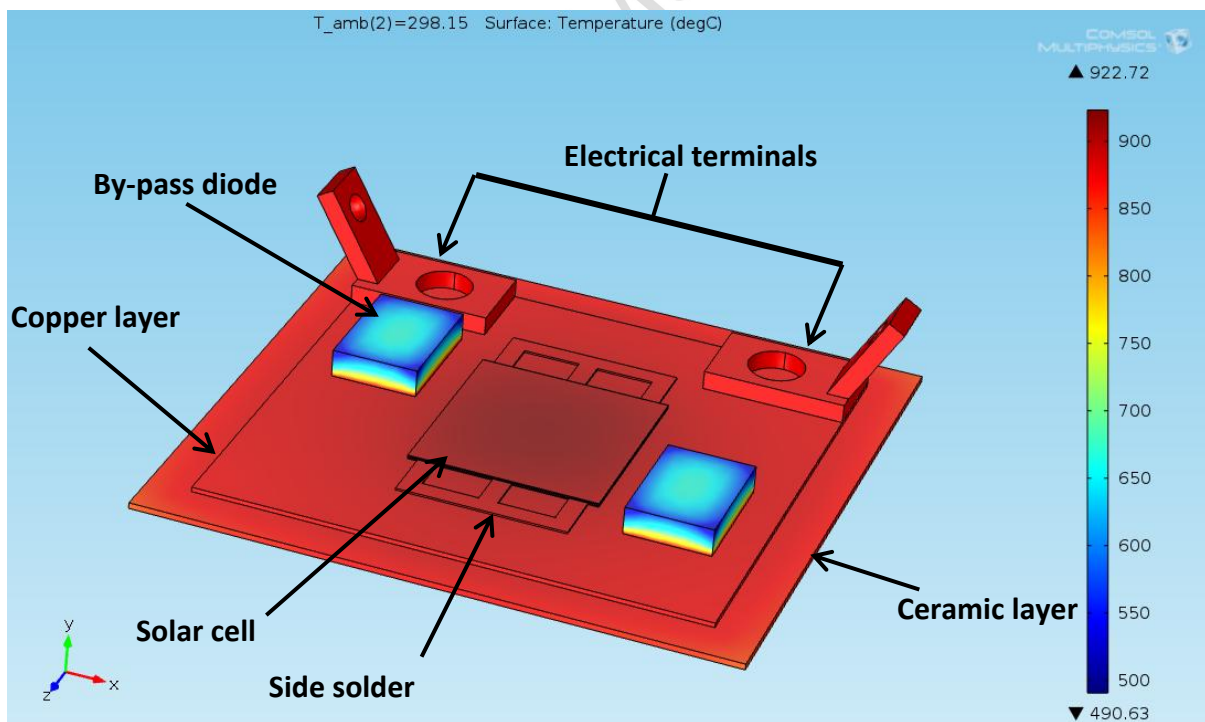
Fig.6: PV assembly temperature distribution for solar cell without heat sink at 25°C ambient temperature

20
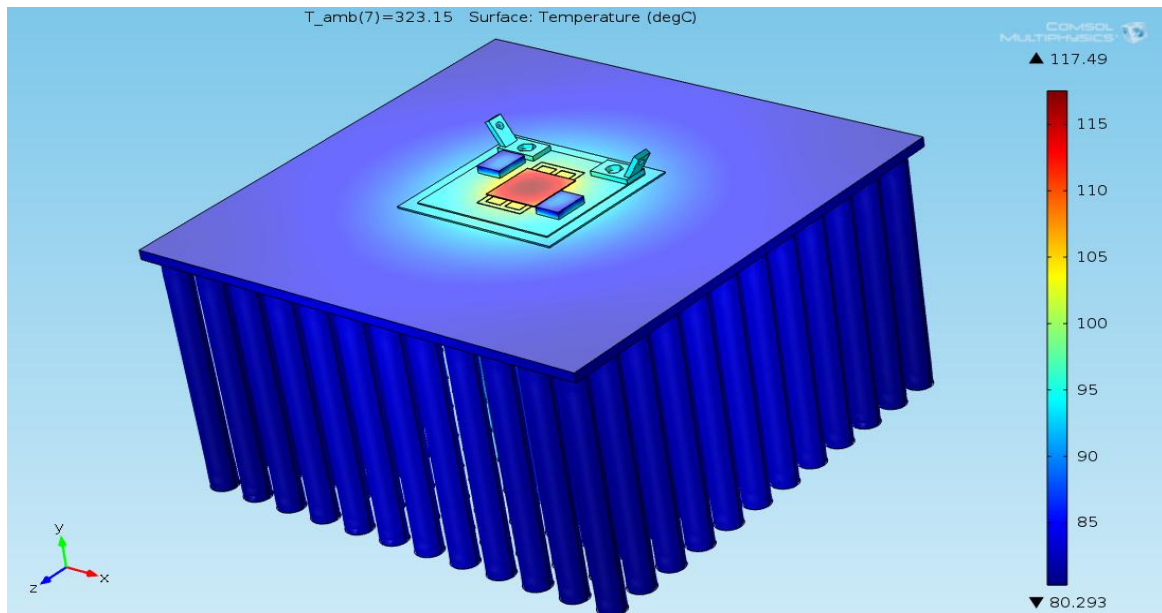
Fig.7: PV temperature profile for RPHS at 50°C ambient temperature
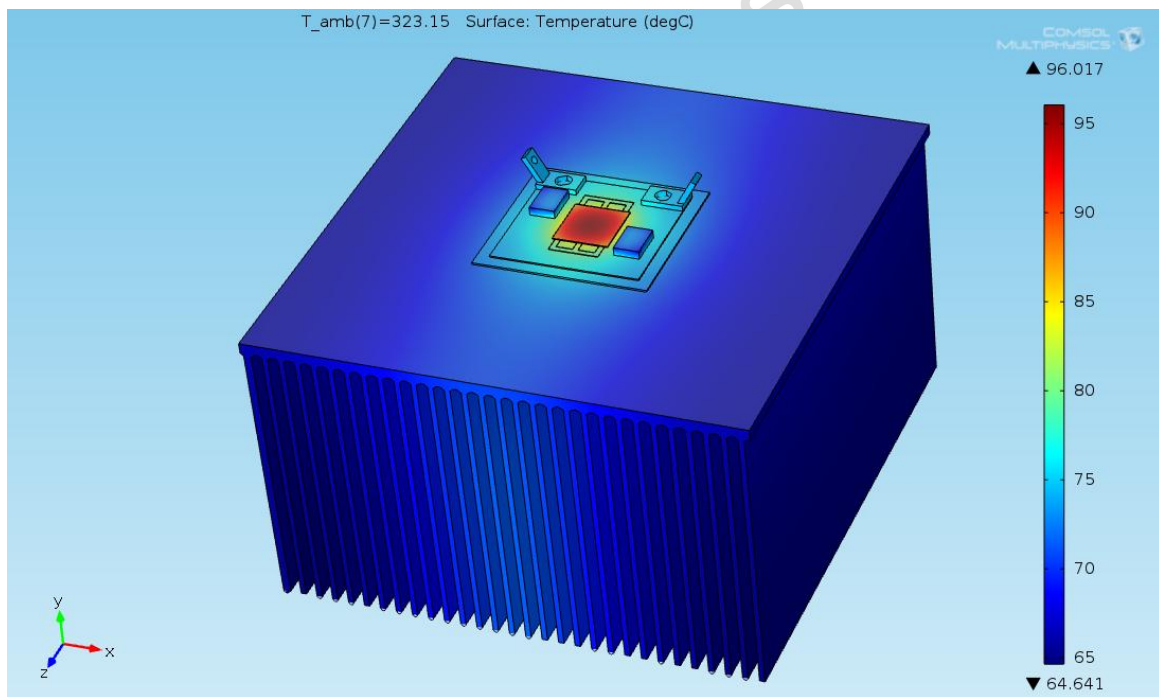
Fig.8: PV temperature profile for SFHS at 50°C ambient temperature
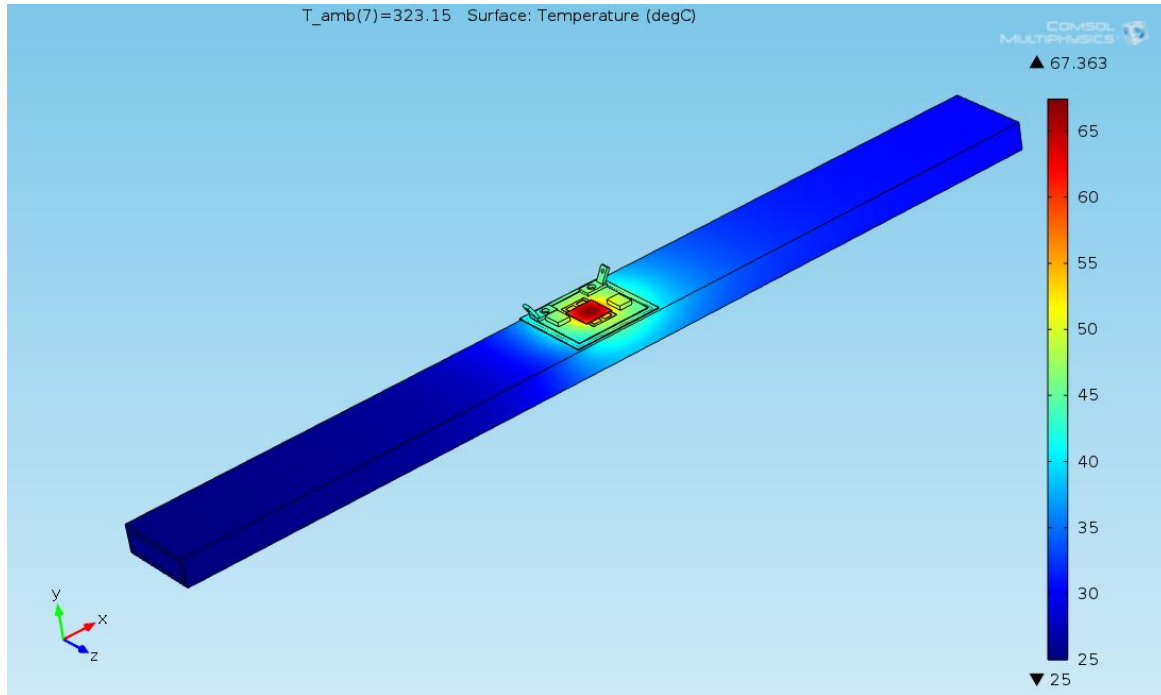
Fig.9: PV temperature profile for active cooling case at 50°C ambient temperature
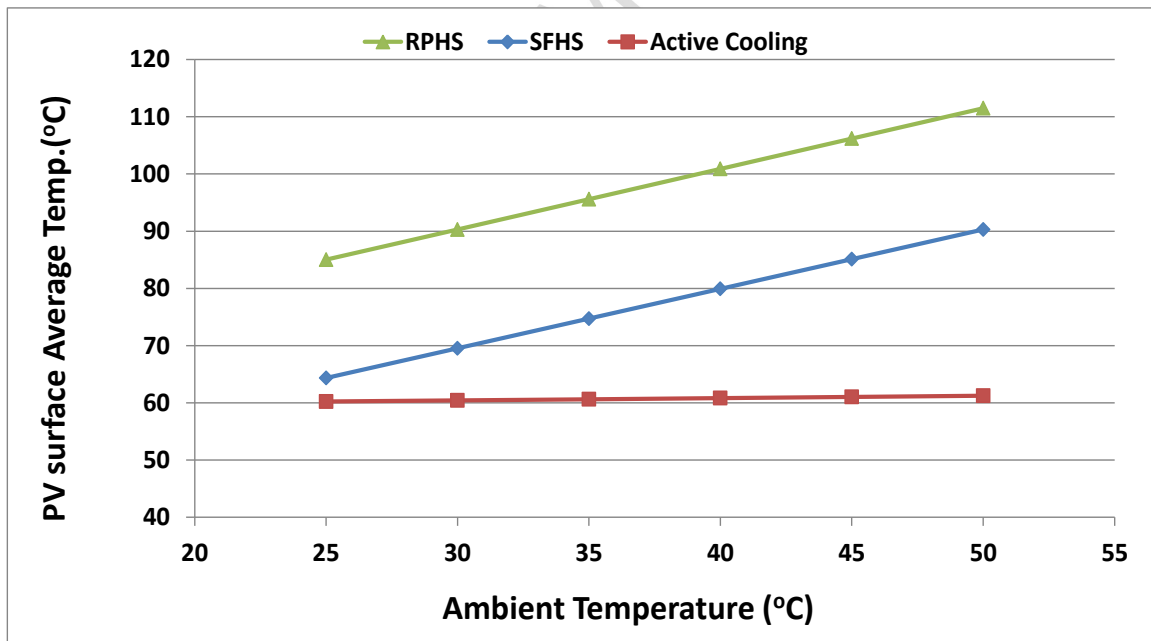
Fig.10: PV average surface temperature at different ambient temperatures
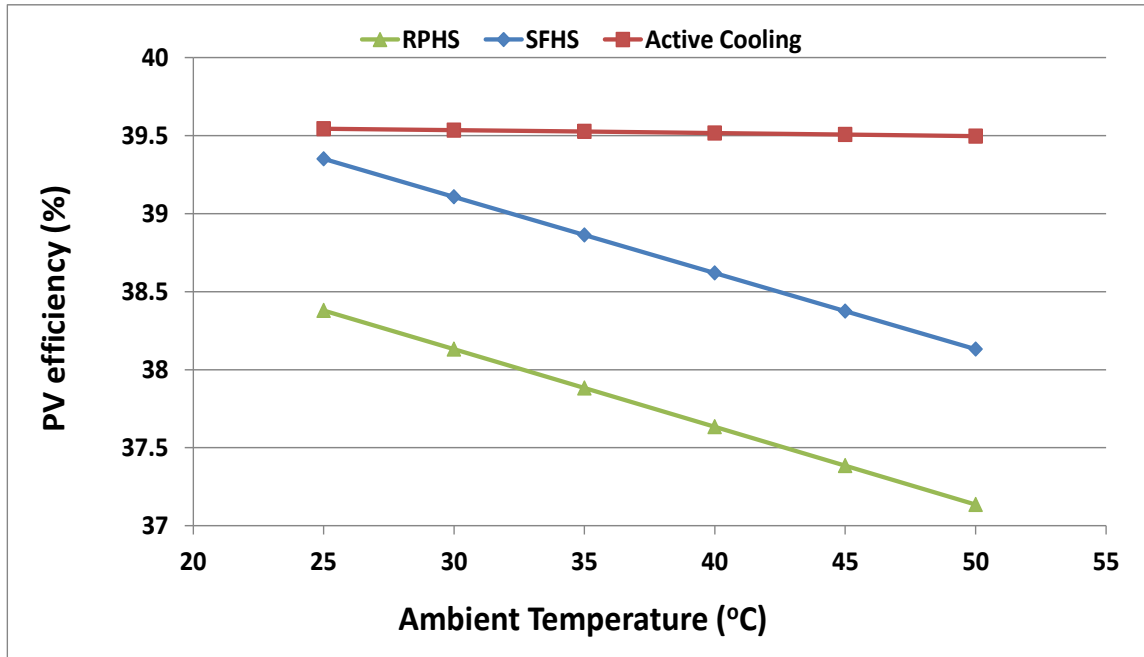
Fig.11: PV efficiency at different ambient temperatures
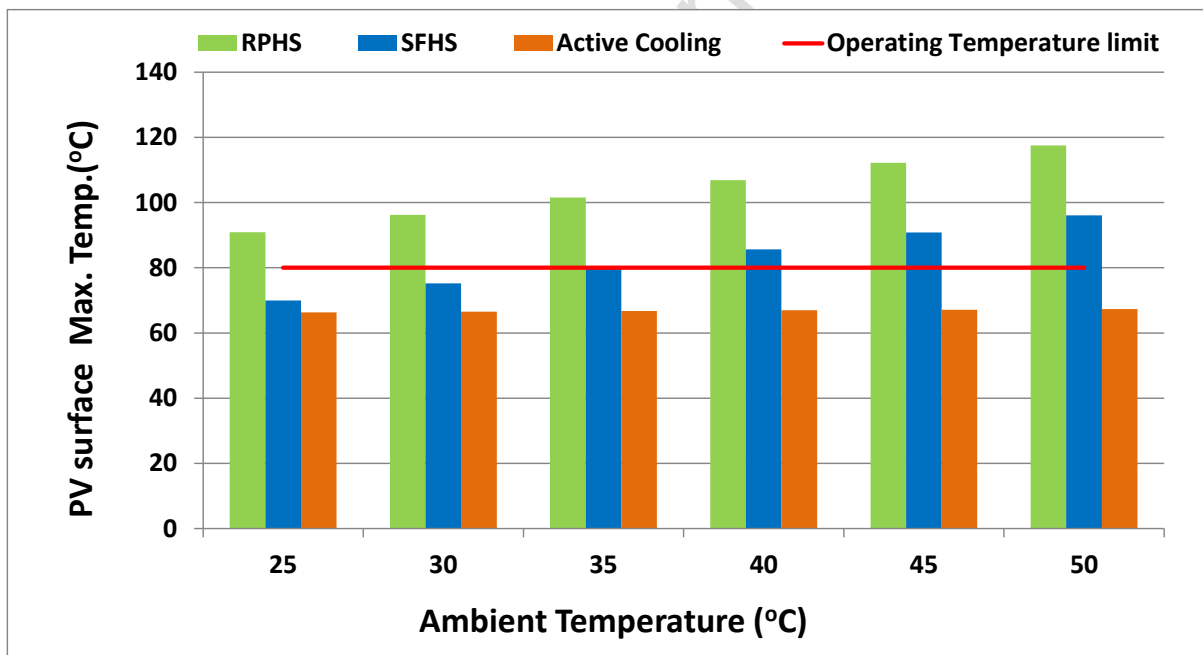
Fig.12: PV surface maximum temperature at different ambient conditions
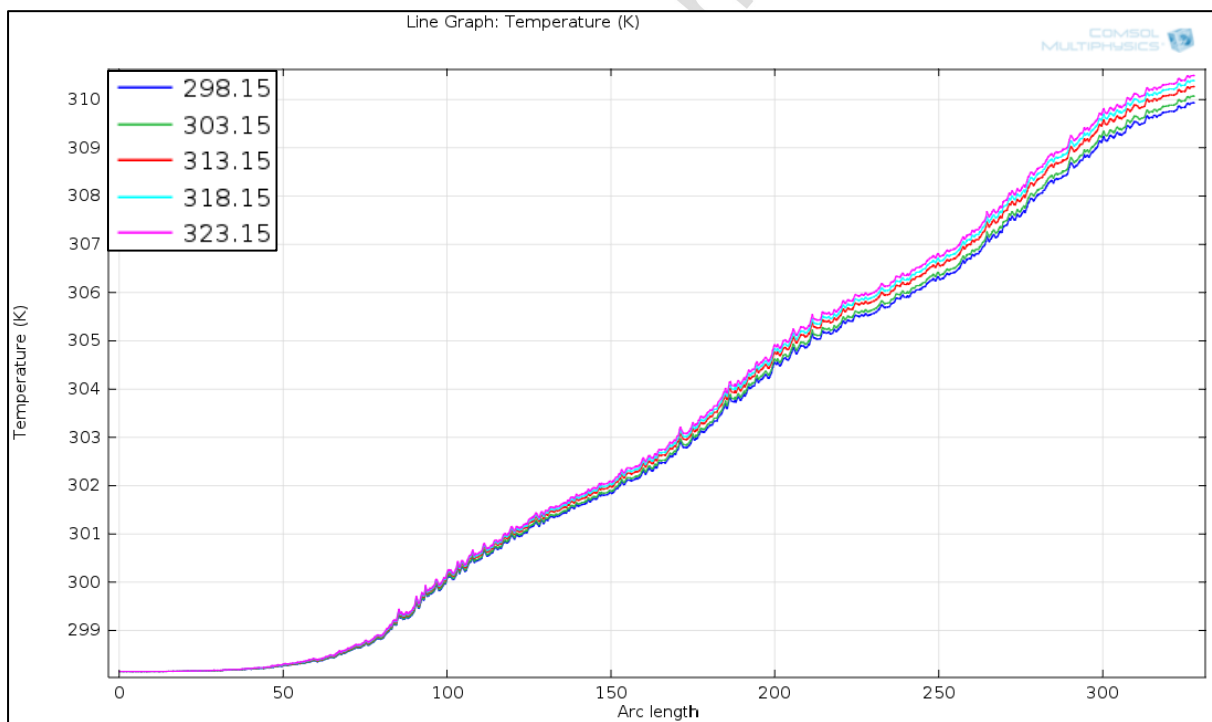
23
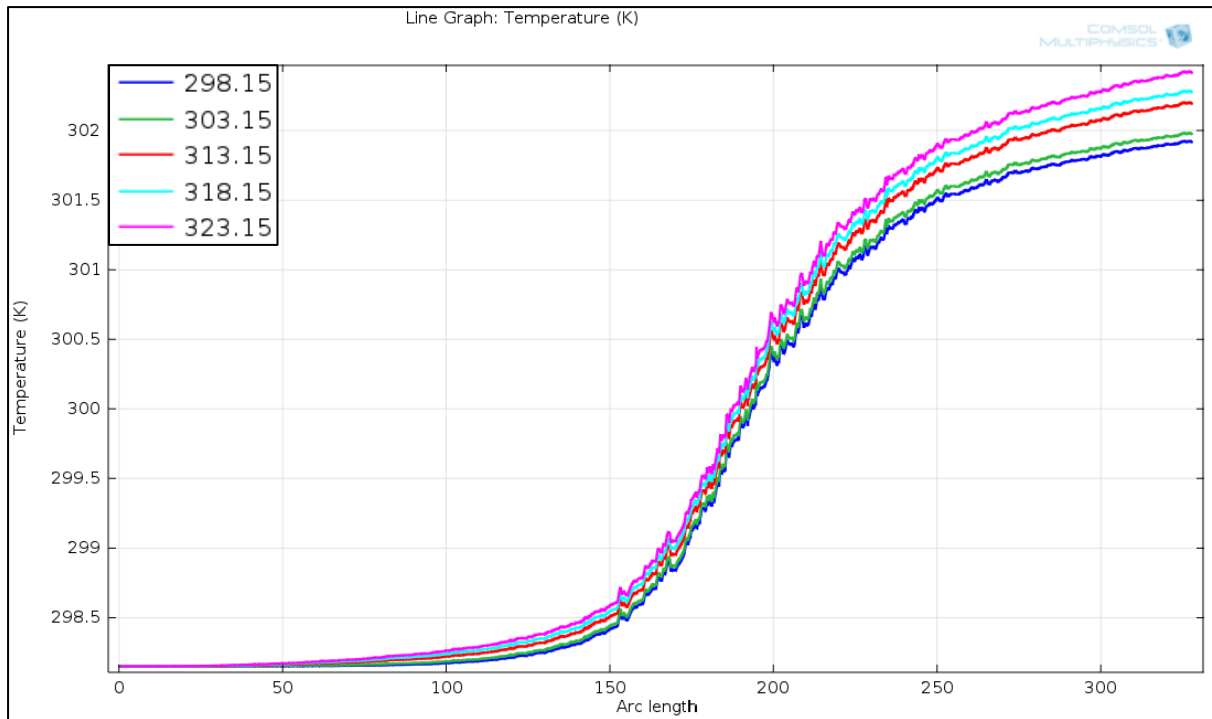
Fig.13: One single CPV water temperature along the cooling channel

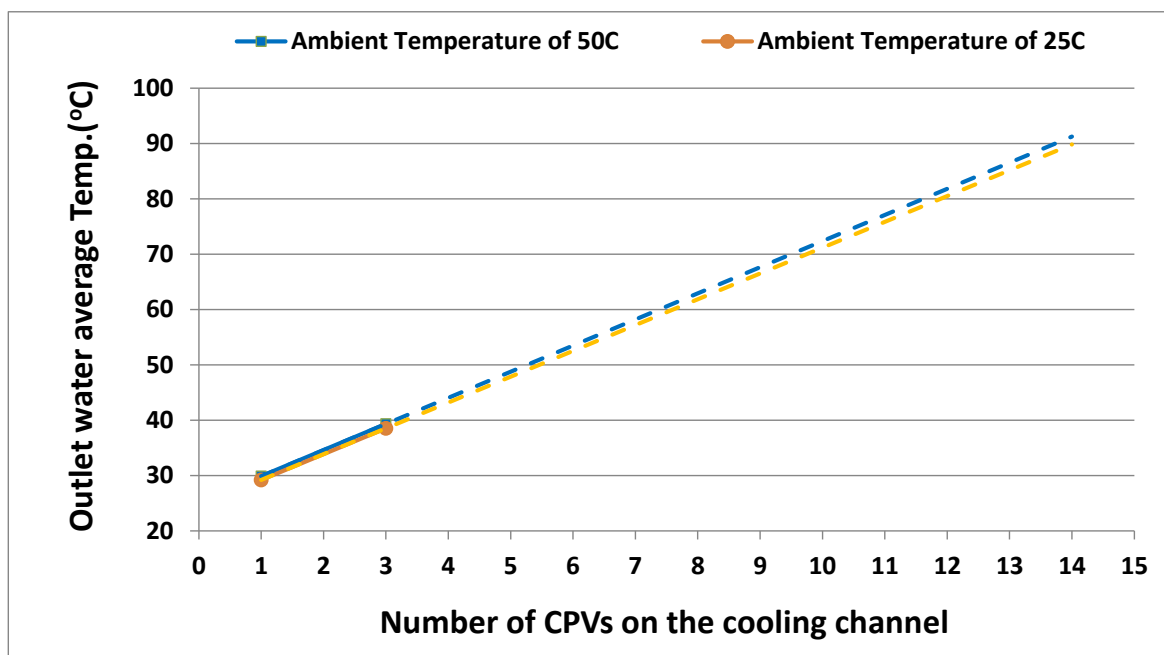Fig.14: Three single CPVs water temperature along the cooling channel

24

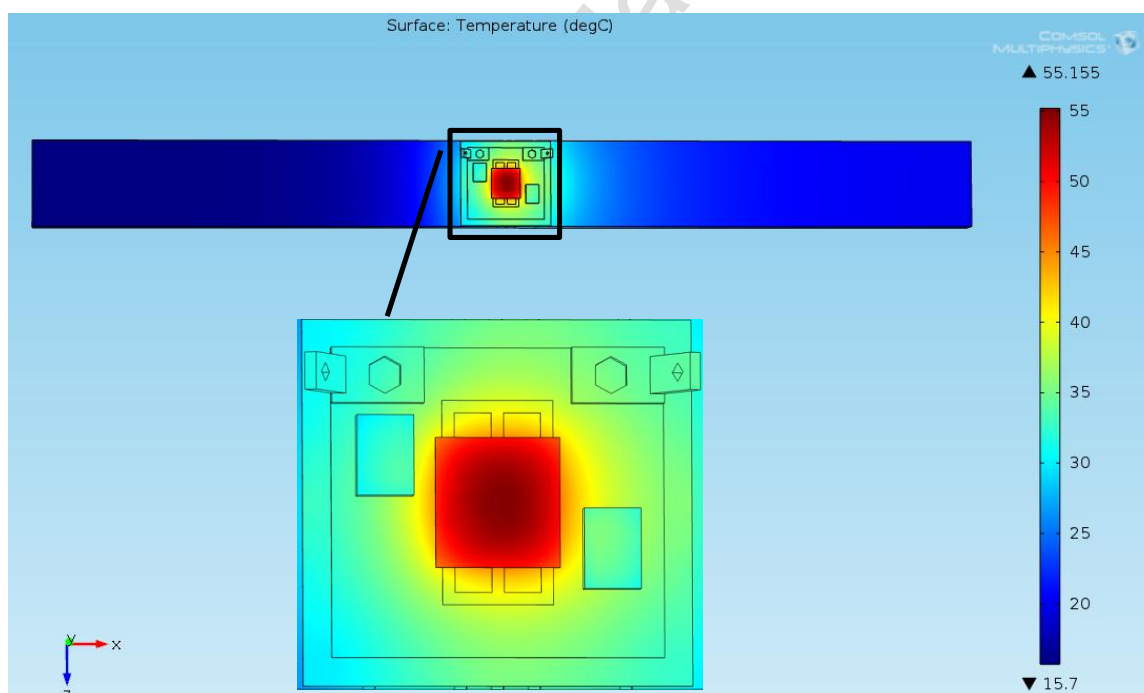Fig.15: Increasing outlet water temperature with number of CPVs

Fig.16: PV temperature profile for active cooling case at 16.9^{o}C ambient temperature and water inlet of 15.7^{o}C
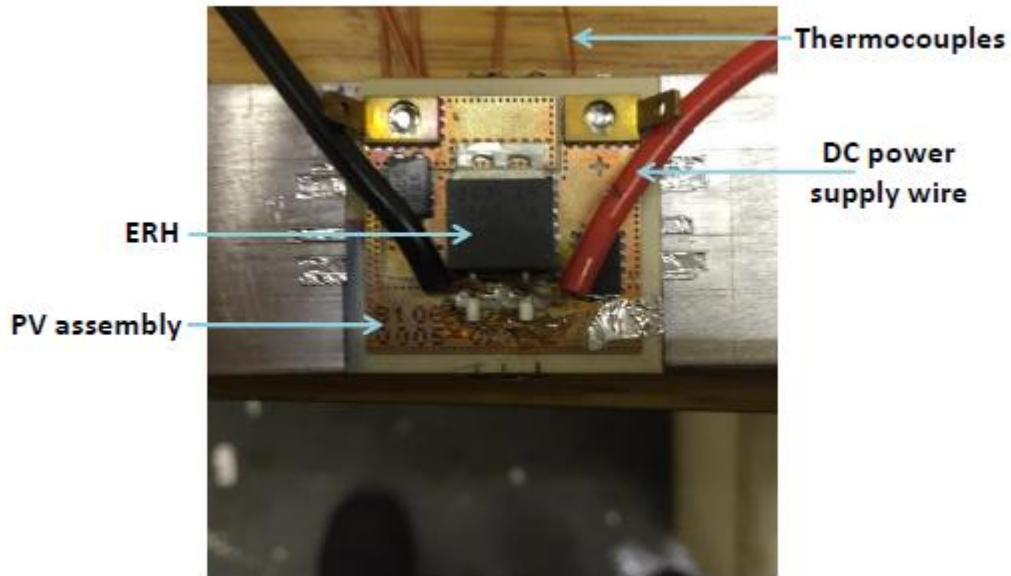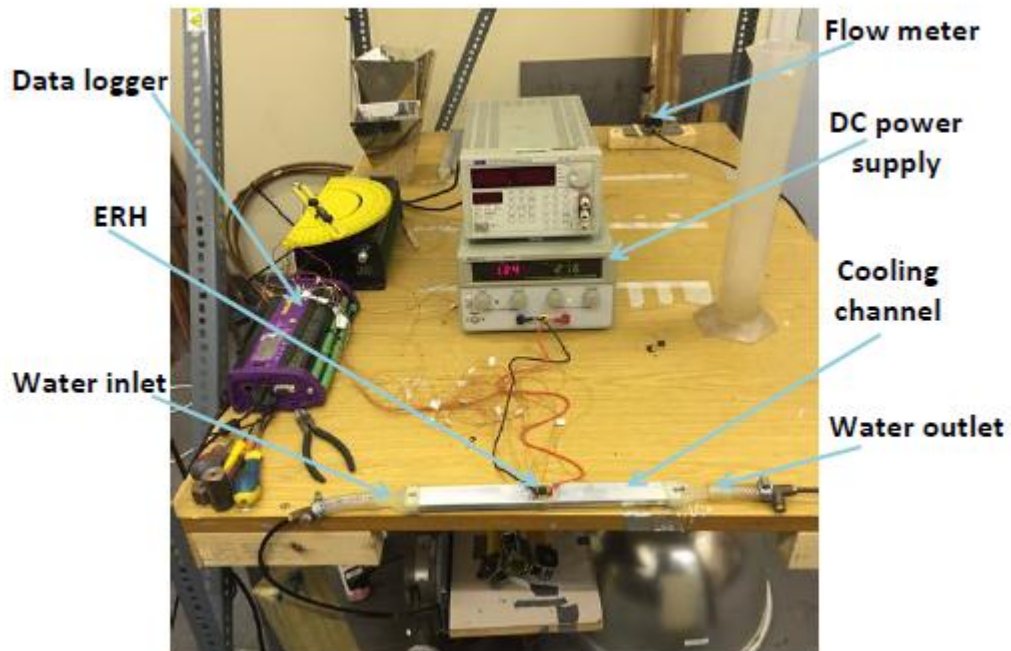
Fig.17: ERH on the top of the PV assembly

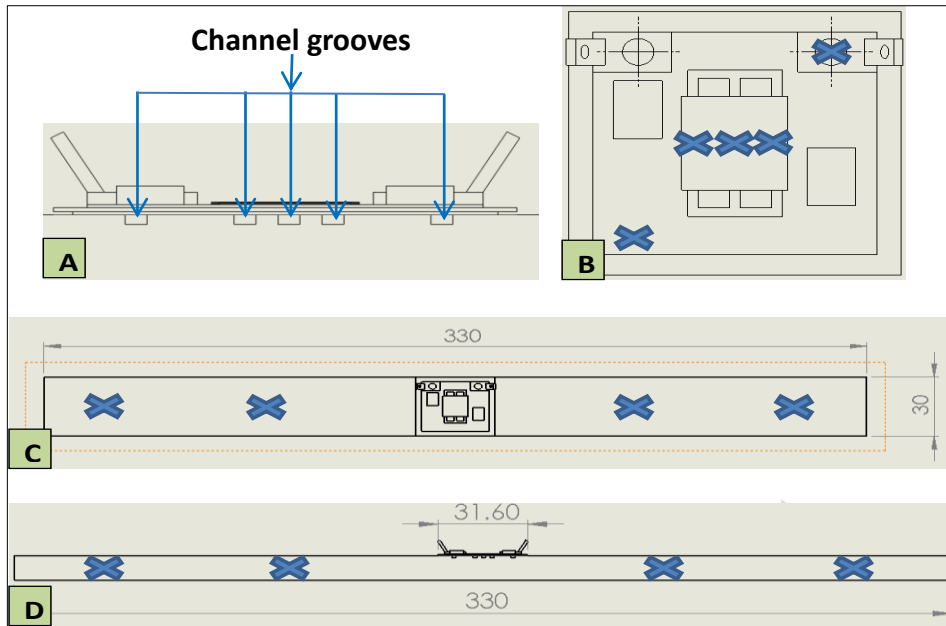Fig.18: Simulation validation experimental set up

26

Fig.19: A: side view of the cooling channel grooves; B: thermocouples locations on the PV assembly; C&D: thermocouples locations at the top and side of the cooling channel
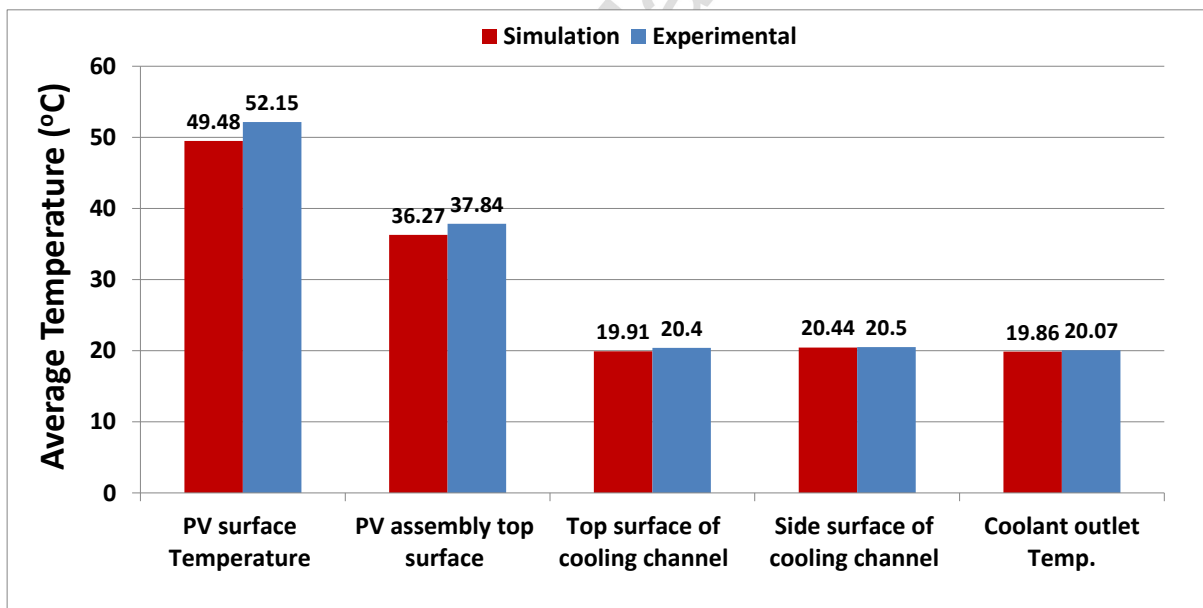

Fig.20: Temperature comparison of the Simulation and the experiment in different CPV locations
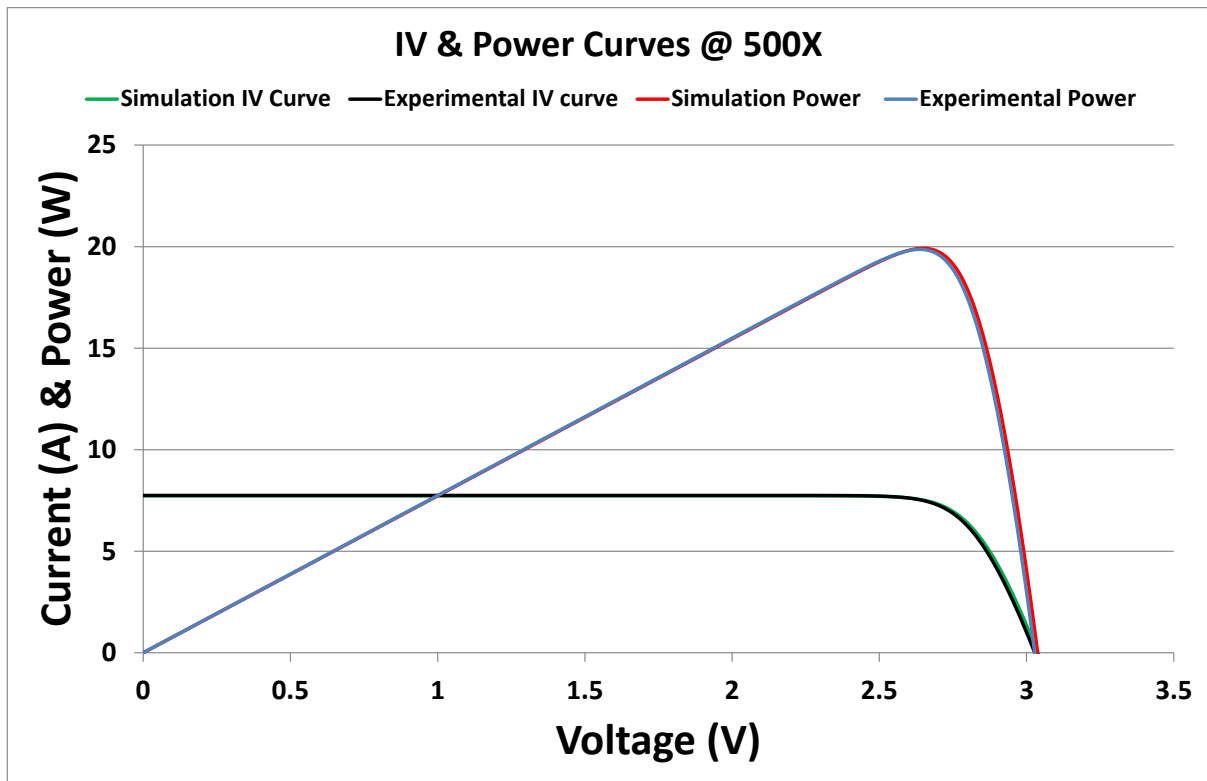
27

Fig.21: IV & Power curves comparison between the experimental and the simulation

Layer	Dimension [mm]	Thickness [mm]
GaInP	10x10	0.066
GaInAs	10x10	0.067
Ge	10x10	0.067
Copper-1	27x25	0.250
Al_2O_3 Ceramic	31.6x29.6	0.320
Copper-2	29x27	0.250
Thermal paste	29x27	0.300

Table1: PV assembly dimensions

Layer	Thermal Conductivity [W/mK]	Heat Capacity [J/kgK]	Density [kg/m^3]
GaInP	73	73	5300
GaInAs	5	300	5500
Ge	60	310	5323
Copper	400	385	8700
Al_2O_3 Ceramic	20	880	3700
Thermal paste	10	800	4000
Aluminium	160	900	2700
Terminal Brass	151	380	8800
Side Solder	50	150	9000
By-pass diode	0.1	700	2329

Table2: thermo-physical properties of PV assembly layers

Ambient Temperature (^{o}C)	System generated heat (W)	Convection to the ambient (W)	Radiation to the ambient (W)	Energy carried by the coolant (W)
25	30.228	1.004	0.023	29.201
30	30.232	0.278	0.021	29.933
35	30.237	-0.498	0.018	30.717
40	30.242	-1.370	0.015	31.597
45	30.247	-2.336	0.012	32.571
50	30.252	-3.361	0.009	33.604

Table3: thermal energy extracted by the coolant fluid

Received power by PV (W)	PV surface average Temp. (^{o}C)	Electrical efficiency (%)	Electrical power output (W)	Thermal power generated (W)
50	49.48	40.05	20.03	29.97

Table4: thermal energy extracted by the coolant fluid

30